JACS
JOURNAL OF THE AMERICAN CHEMICAL SOCIETY

Article

pubs.acs.org/JACS

Molecular Design for Dual Modulation Effect of Amyloid Protein Aggregation

Lijuan Zhu,† Yang Song,† Pin-Nan Cheng,* and Jeffrey S. Moore*

Department of Chemistry and Materials Research Laboratory, University of Illinois at Urbana−Champaign, Urbana, Illinois 61801, United States

Supporting Information

ABSTRACT: Modulation of protein self-assembly has been a powerful strategy for controlling and understanding amyloid protein aggregation. Most modulators of amyloid aggregation only involve simple inhibition or acceleration. Here we report a new multivalent molecular motif, the polyethylenimine−perphenazine (PEI-P) conjugate which has a dual "acceleration−inhibition" modulation effect on amyloid β (Aβ) aggregation. Dose dependent results from Thioflavin T fluorescence assays, circular dichroism, and atomic force microscopy show that PEI-P conjugates *accelerate* formation of Aβ prefibrillar intermediates and then *inhibit* Aβ fibrillation. Furthermore, compared to perphenazine alone, PEI-P conjugates exhibit an enhanced inhibitory effect due to multivalency. Cell viability assays indicate that the PEI-P conjugates reduce the cytotoxicity of Aβ aggregates in a dose-dependent manner. This new modulation strategy may shed light on controlling amyloid aggregation, which offers a general concept for designing new modulators.

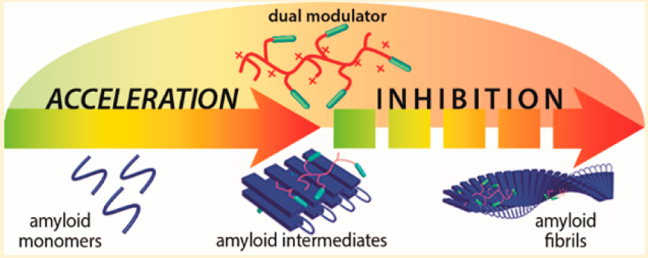

INTRODUCTION

Molecular self-assembly is a universal event in nature, where it is central to the formation of a variety of complexes with ordered structures.[1] Amyloid protein aggregation is a fibrillar self-assembly process governed by a nucleation-dependent polymerization, in which the formation of oligomeric intermediates and nuclei is slow, and the approach to critical-size nuclei is rate determining (Figure 1a).[2] The ultimate products of amyloid aggregation are insoluble long, unbranched proteinaceous fibrils, called amyloid fibrils. Extensive studies indicate that elusive oligomeric intermediates, rather than the most visible amyloid fibrils, are the cause of cytotoxicity in amyloid aggregation and the pathological species of Alzheimer's disease (AD).[3] Although literature has reported that amyloid fibrils and intermediates from AD brain tissue exhibit key differences from those *in vitro*,[4] extensive research has applied the *in vitro* Aβ fibrillation models to design modulators for amyloid aggregation, which provide insight and understanding for the mechanism of amyloid protein aggregation as well as the potential foundation for promising solutions to investigate Alzheimer's disease.[5] To control amyloid aggregation, modulation of various steps of fibrillar growth provides a promising strategy.[6] Modulators of fibrillar growth can regulate the final size and shape of noncovalent protein assemblies, while potentially transforming the cytotoxic properties of the aggregation products.[7] The current modulation of amyloid aggregation by modulators mainly includes inhibition and acceleration, as summarized below.

Inhibition has been an effective strategy to modulate the process of amyloid aggregation.[8] Inhibitory modulation is usually used to prevent amyloid fibril formation and thus reduce cytotoxic effects of amyloid aggregates (Figure 1b). Many inhibitory modulators, including small molecule-,

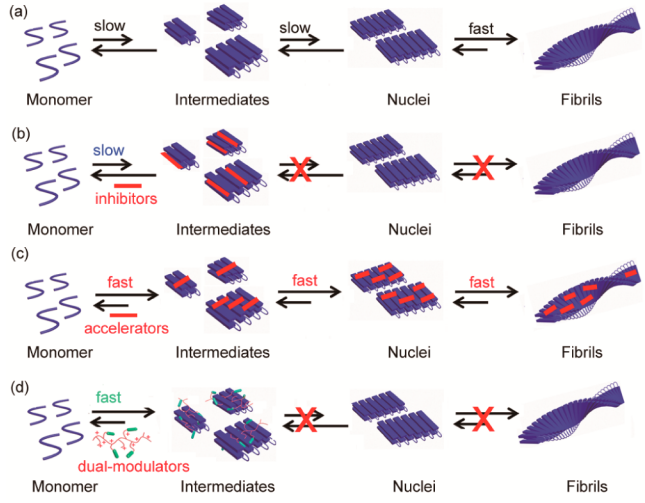

Figure 1. Cartoon representation of simplified amyloid protein aggregation without (a) and with (b−d) modulators. (a) Amyloid protein aggregation governed by a nucleation-dependent polymerization. (b) Inhibition of amyloid protein aggregation by an inhibitor. (c) Acceleration of amyloid protein aggregation by an accelerator. (d) Dual modulation of amyloid protein aggregation by a dual modulator.

Received: July 7, 2014
Published: June 4, 2015

DOI: 10.1021/jacs.5b01651
J. Am. Chem. Soc. 2015, 137, 8062−8068

peptide-, nucleic acid-, antibody-, and nanomaterial-based inhibitors, have been developed and studied.[9] For example, small molecules such as curcumin, Congo red, inositols, polyphenols, and peptide-based inhibitors were used to effectively inhibit aggregation of various amyloid proteins, e.g., tau, huntingtin, α-synuclein, transthyretin, and amyloid β (Aβ).[10] By controlling amyloid aggregation, researchers will have the tools to elucidate the molecular etiology of disease associated with protein aggregation in *in vitro* studies.[5]

Recently, acceleration has become a promising strategy to modulate the process of amyloid aggregation (Figure 1c).[11] The Wanker group demonstrated that the orcein-related small molecule O4 stabilizes the aggregated Aβ intermediates and promotes the aggregation process.[11] Consequently, the accelerated removal of Aβ aggregates converts toxic Aβ oligomers to nontoxic Aβ fibrils. This seminal work showed that acceleration has a clearing capability with therapeutic potential. It is clear that inhibitory and acceleratory modulation have provided powerful approaches to understand and control amyloid protein aggregation. However, these are the only two modulation approaches known at present.

Since a new type of modulation scheme might usher in breakthroughs in controlling protein aggregation and provide new design concepts in amyloid aggregation,[12] we asked whether there is an alternative approach to modulate the amyloid aggregation. Attempts to develop a new modulation approach involve a promising design of multifunctional modulators which target multiple regions on amyloid proteins.[13] However, multifunctional modulators have rarely been reported to target different phases along the amyloid protein aggregation pathway. Here, we provide evidence for a new multifunctional modulation concept, a dual modulation that includes both acceleration and inhibition of amyloid aggregation (Figure 1d). Compared to the simple inhibition or acceleration, this dual modulation presents an alternative strategy to stabilize transient intermediates, which may shed light on mechanism studies on amyloid aggregation as well as a potential foundation to investigate the pathogenic species formed from the aggregation pathway. To realize this modulation concept, we chose the well-studied Aβ peptide as a model system and targeted a new molecular design for dual-effect behavior. As shown below, polyethylenimine–perphenazine (PEI-P) conjugates act as dual-effect modulators which both accelerate and inhibit the process of Aβ aggregation. The PEI-P conjugates comprise a positively charged PEI core that accelerates through Coulombic interactions. This acceleration core is further decorated with multiple copies of perphenazine, a small molecule inhibitor, to form an inhibitory periphery. Therefore, PEI-P conjugates are dual-effect modulators with acceleratory and inhibitory components (Figure 2). Thioflavin T (ThT) fluorescence, atomic force microscopy (AFM), and circular dichroism (CD) studies show that the PEI-P conjugates first accelerate the early structural transformation of prefibrillar Aβ intermediates and then inhibit Aβ fibrillation. Furthermore, our MTT studies show that Aβ aggregates mediated by PEI-P conjugates are accompanied by a reduction of Aβ cytotoxicity. We envision that the present dual-effect modulation strategy will provide an alternative design concept for manipulating aggregation of different amyloid proteins and may provide insights into amyloid aggregation that cannot be obtained by simple inhibition or acceleration alone.

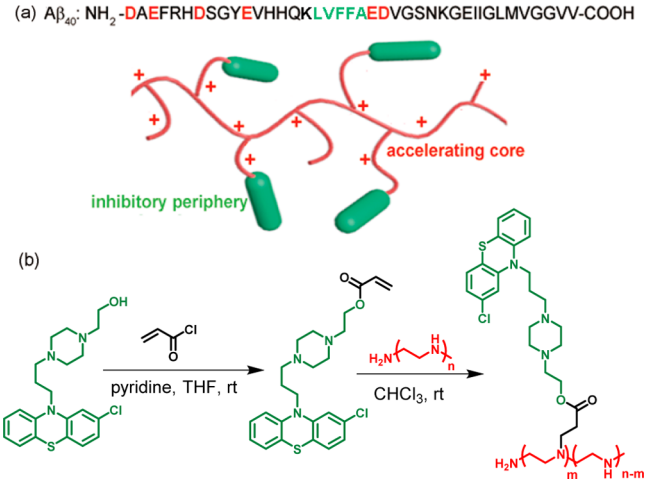

Figure 2. Design and synthesis of polyethylenimine–perphenazine conjugates. (a) Amino acid sequences of Aβ_{40} in which the negatively charged amino acid residues at pH 7.4 are in red, while the central hydrophobic residues are in green. Design of PEI-P conjugates in which the positively charged PEI core at pH 7.4 is in red, while the peripheral perphenazines are in green. (b) Synthesis of PEI-P conjugates.

RESULTS

Design and Synthesis of Dual-Effect Modulators. The polyethylenimine–perphenazine conjugates with a PEI core (M_n: 600, M_w: 800) attached to multiple copies of perphenazine inhibitors were rationally designed to achieve the dual effect on Aβ aggregation (Figure 2a). Recent work shows that cellular polyamines, a family of small molecule polycationic alkylamines, accelerate Aβ aggregation by targeting the negatively charged *N*-terminus of Aβ protein (Figure 2a, marked in red).[14] In addition, positively charged PEI was also reported to accelerate α-synuclein fibrillation associated with Parkinson's disease.[15] Analogously, we expected that the PEI core will also accelerate Aβ aggregation. Perphenazine, an aromatic small molecule, is a known inhibitor of Aβ aggregation, so we envisioned that attachment of perphenazines to the periphery will inhibit Aβ aggregation via targeting hydrophobic residues of Aβ sequences (LVFFA).[16]

The PEI-P conjugates were prepared in two steps (Figure 2b). Perphenazine-acrylate was first synthesized by the nucleophilic substitution of the acryloyl chloride with perphenazine. Michael addition of the perphenazine-acrylate to the commercially available branched PEI, containing, on average, 14 repeating units of [CH_2CH_2NH] produced conjugates with a molar ratio of 4.5:1 (moles of perphenazine-acrylate per mole of PEI oligomer). The composition was determined by NMR. We use the notation PEI-P-4.5 to designate the small molecule loading of the conjugate.

Modulation of Aβ Aggregation by PEI, Perphenazine, and PEI-P Conjugates. To investigate the modulation effects of PEI, perphenazine, and PEI-P-4.5 on Aβ_{40} aggregation, we used the lag phase measured by ThT fluorescence assays to first evaluate their activities against Aβ_{40} (15 μM) aggregation.[17] AFM studies were used to corroborate the results from the ThT assays. The ThT assays show that PEI accelerates Aβ_{40} aggregation by 44% at 0.13 equiv (i.e., molar ratio of PEI oligomer to Aβ_{40}), decreasing the lag time from 190 to 105 min (Figure S36b) and by 58% at 1.3 equiv, decreasing the lag time from 190 to 80 min (Figure 3b). As a control, PEI alone in the

DOI: 10.1021/jacs.5b01651
J. Am. Chem. Soc. 2015, 137, 8062–8068

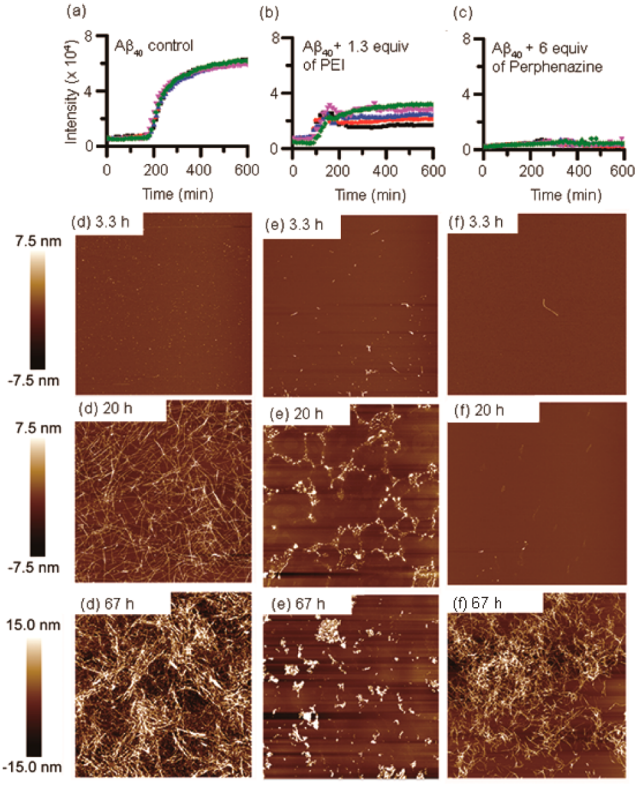

Figure 3. ThT fluorescence assays and AFM images. (a) Fibrillation kinetics of Aβ_{40} (15 μM) monitored by a ThT fluorescence assay. ThT fluorescence assays of Aβ_{40} aggregation with 19.5 μM of PEI, 1.3 equiv (b), and 90 μM of perphenazine, 6 equiv (c). ThT assays were performed on 15 μM Aβ_{40} peptide in HEPES buffer (pH 7.4) at 37 °C. For clarity of the lag phase, the ThT fluorescence assay data in (a)−(c) are plotted only for the first 10 h out of the full time course (67 h). For the complete ThT data in the full time course, see Figure S31. AFM images of Aβ_{40} (15 μM) after incubation for 3.3, 20, and 67 h without modulators (d), and with 19.5 μM of PEI, 1.3 equiv (e), and 90 μM of perphenazine, 6 equiv (f). Samples for AFM studies were taken directly from the ThT assays. Image size is 10 × 10 μm^2. We define equiv as molar ratio of PEI oligomer or perphenazine to Aβ_{40}.

absence of Aβ_{40} has no ThT fluorescence response (Figure S32). These results indicate that the acceleratory effect of PEI is not strongly dose-dependent. Surprisingly, AFM studies of samples taken from the ThT assays show that PEI accelerates formation of disordered aggregates, rather than long unbranched mature fibrils (Figure S36e and 3e). These results suggest that PEI interacts with Aβ_{40} or Aβ_{40} aggregates to alter the association of Aβ_{40} monomers that would otherwise lead to final fibril formation. The intermolecular interaction between PEI and Aβ_{40} is supported by zeta potential measurements (Figure S44). The above results demonstrate that PEI first accelerates the early structural transformation of prefibrillar Aβ intermediates and then redirects Aβ aggregation to form disordered aggregates.

ThT assays also show that perphenazine inhibits Aβ_{40} aggregation in a dose-dependent manner (Figure S29). For example, perphenazine does not significantly affect Aβ_{40} aggregation at 0.6 equiv (Figure S36c), but delays Aβ_{40} aggregation at 6 equiv (Figure 3c). These results are confirmed by the AFM studies (Figures S36f and 3f). AFM images show that Aβ_{40} forms fibrils in the presence of perphenazine (0.6 equiv), indicative of no significant effect on Aβ_{40} fibrillation (Figure S36f). Aβ_{40} does not form fibrils in the presence of perphenazine (6 equiv) after 20 h of incubation during the delayed lag time, indicative of inhibition of Aβ_{40} fibrillation (Figure 3f, middle). The delayed Aβ40 aggregation in the presence of perphenazine (6 equiv) is also confirmed by micro-DSC thermograms (Figure S43). However, the prefibrillar Aβ_{40} intermediates stabilized by perphenazine (6 equiv) eventually yield fibril formation after 67 h of incubation (Figure 3f, bottom).

Interestingly, ThT fluorescence assays and AFM studies indicate that the PEI-P-4.5 conjugate modulates Aβ_{40} aggregation in a dose-dependent manner (Figure 4b and 4c).

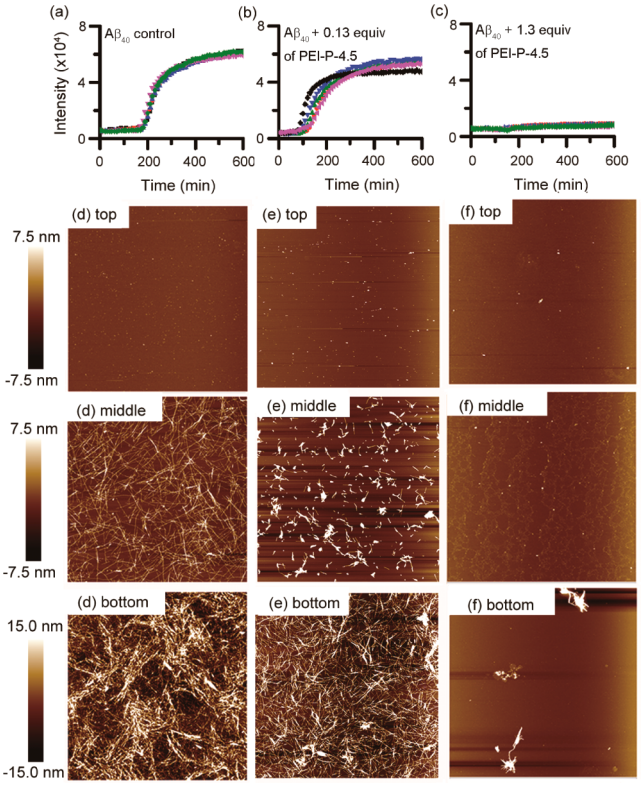

Figure 4. ThT fluorescence assays and AFM images. (a) Fibrillation kinetics of Aβ_{40} monitored by a ThT fluorescence assay. ThT fluorescence assays of Aβ_{40} aggregation with 1.95 μM of PEI-P-4.5, 0.13 equiv (b), and 19.5 μM of PEI-P-4.5, 1.3 equiv (c). ThT assays were performed on 15 μM Aβ_{40} peptide in HEPES buffer (pH 7.4) at 37 °C. For clarity of the lag phase, the ThT fluorescence assay data in (a)−(c) are plotted only for the first 10 h out of the full time course (67 h). For the complete ThT data in the full time course, see Figure S31. AFM images of Aβ_{40} (15 μM) after incubation for 3.3, 20, and 67 h without modulators (d), and with 1.95 μM of PEI-P-4.5, 0.13 equiv (e), and 19.5 μM of PEI-P-4.5, 1.3 equiv (f). Samples for AFM studies were taken directly from the ThT assays. Image size is 10 × 10 μm^2. We define equiv as the molar ratio of PEI-P-4.5 oligomer to Aβ_{40}.

PEI-P-4.5 at the lower concentration (0.13 equiv, define as the molar ratio of PEI-P-4.5 oligomer to Aβ_{40}) exhibits a dual effect on modulation of Aβ_{40} aggregation, while PEI-P-4.5 at the higher concentration (1.3 equiv) acts more like an inhibitor. ThT fluorescence assays show that PEI-P-4.5 (0.13 equiv) accelerates Aβ_{40} aggregation by 41%, decreasing the lag time from 190 to 110 min (Figure 4b). The acceleration effect of PEI-P-4.5 is similar to that of PEI. However, unlike the promotion of the off-pathway Aβ_{40} aggregation by PEI, AFM

DOI: 10.1021/jacs.5b01651
J. Am. Chem. Soc. 2015, 137, 8062−8068

studies indicate that PEI-P-4.5 promotes an on-pathway aggregation which ultimately leads to fibrillation (Figure 4e). These results provide evidence that PEI-P-4.5 at the low concentration is able to accelerate the formation of the prefibrillar Aβ_{40} intermediates and delay Aβ_{40} fibrillation. It is suggested that the prefibrillar Aβ_{40} intermediates promoted by PEI-P-4.5 (0.13 equiv) and PEI (0.13 equiv) are different because one is on the pathway of Aβ_{40} fibrillation, while the other is not. ThT assays also show that the fibrillation kinetics of Aβ_{40} aggregation with PEI-P-4.5 (1.3 equiv) does not shorten the lag time which is indicative of an acceleration effect; instead, it exhibits a delayed lag phase (Figure 4c). AFM studies confirm that Aβ_{40} does not form fibrils in the presence of PEI-P-4.5 (1.3 equiv) even after 67 h of incubation (Figure 4e).

To understand the different modulation effects of PEI-P conjugates and the mixture of PEI and perphenazine on Aβ_{40} aggregation, we use ThT and AFM to investigate the aggregation process. ThT assays show that the lag times of Aβ_{40} incubated with 0.13 equiv of PEI alone and PEI plus 0.2, 0.4, and 0.6 equiv of perphenazine are 94 ± 5.5, 68 ± 8.4, 70 ± 7.1, and 66 ± 8.9 min, while the lag times of Aβ incubated with 1.3 equiv of PEI alone and PEI plus 2, 4, and 6 equiv of perphenazine are 78 ± 5.5, 72 ± 4.5, 68 ± 4.5, and 62 ± 4.5 min (Figure S35, Table S2, Table S4). Unlike the modulation behavior of the PEI plus perphenazine mixture, PEI-P conjugates show a shorter lag time at 0.13 equiv while no obvious lag phase at 1.3 equiv (Figure 4).

From AFM data, we found that when Aβ_{40} was coincubated with the mixture of PEI and perphenazine, small aggregates formed after 3.3 h of incubation, which is attributed to the acceleration effect of PEI (Figure 5d, 3.3 h; e, 3.3 h; and f, 3.3 h). After 20 h of incubation, AFM studies of samples taken from the ThT assays show much more disordered aggregates (Figure 5d, 20 h; e, 20 h; and f, 20 h). However, the modulation effects of PEI plus perphenazine with different concentrations do not show an obvious difference, whose modulations are more like the modulation behavior of PEI. In addition, the AFM results indicate that PEI-P-4.5 (1.3 equiv), compared to perphenazine (6 equiv) and the mixture of PEI and perphenazine, exhibits an enhanced activity against Aβ_{40} aggregation. This enhanced activity may result from the multivalent effect.

To further investigate the effects of the PEI, perphenazine, and PEI-P-4.5 on the early transition of Aβ_{40} aggregation, we turned to CD studies which are extensively used to probe secondary structures of polypeptides and provide a means to monitor the structural conversion over a period of time.[18] When Aβ_{40} was incubated to aggregate, we intentionally reduced the intensity of shaking (from 567 rpm for ThT assays to 100 rpm for CD) to increase the lag phase, so that we could better observe the effects of those modulators on the early stage of Aβ_{40} aggregation. Initially, the CD spectrum of Aβ_{40} (50 μM) aggregation typically displays a curve with a negative peak at 198 nm, which is characteristic of random coils. As Aβ_{40} continues to aggregate, the intensity of the negative peak at 198 nm gradually diminishes over 45 h, and a new curve forms with a positive peak emerging around 194 nm and a negative peak around 217 nm (Figure 6a). The change of the CD spectra indicates the conformational conversion of Aβ_{40} from random coils to β-sheets and thus suggests the formation of Aβ_{40} fibrils. Our CD results are consistent with those reported in the literature.[19] The CD studies show that the negative peaks at 198 nm disappear after 4 h of incubation of Aβ_{40} with 1.3 equiv

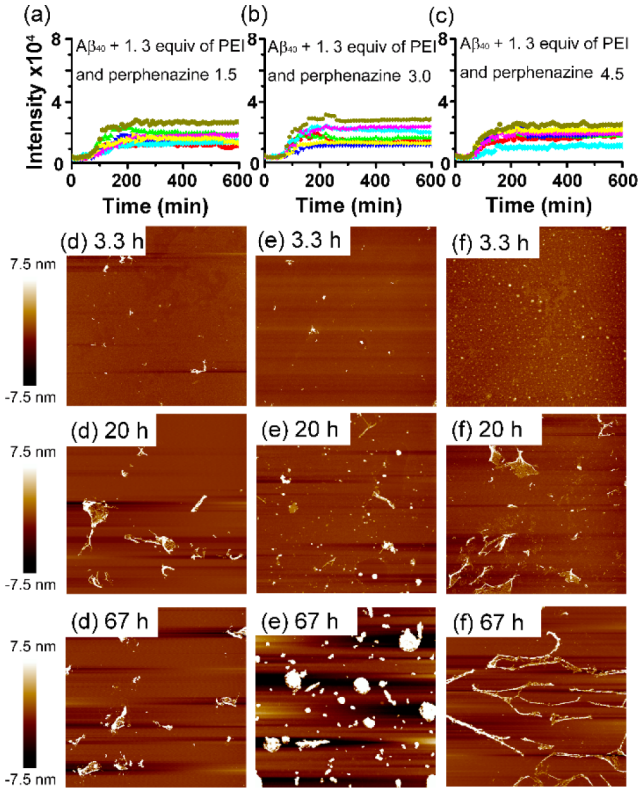

Figure 5. ThT fluorescence assays and AFM images. ThT fluorescence assays of Aβ_{40} aggregation with 19.5 μM of PEI and 30 μM of perphenazine, 1.3 equiv of PEI and 2 equiv of perphenazine (a), 19.5 μM of PEI and 60 μM of perphenazine, 1.3 equiv of PEI and 4 equiv of perphenazine (b), and 19.5 μM of PEI and 90 μM of perphenazine, 1.3 equiv of PEI and 6 equiv of perphenazine (c). ThT assays were performed on 15 μM Aβ_{40} peptide in HEPES buffer (pH 7.4) at 37 °C. For clarity of the lag phase, the ThT fluorescence assay data in (a)−(c) are plotted only for the first 10 h out of the full time course (67 h). AFM images of Aβ_{40} (15 μM) after incubation for 3.3, 20, and 67 h with 19.5 μM of PEI and 30 μM of perphenazine, 1.3 equiv of PEI and 2 equiv of perphenazine (d), 19.5 μM of PEI and 60 μM of perphenazine, 1.3 equiv of PEI and 4 equiv of perphenazine (e), and 19.5 μM of PEI and 90 μM of perphenazine, 1.3 equiv of PEI and 6 equiv of perphenazine (f). Samples for AFM studies were taken directly from the ThT assays. Images size is 10 × 10 μm^2. We define equiv as the molar ratio of PEI plus perphenazine with different concentrations to Aβ_{40}.

of PEI (Figure 6b) and PEI-P (Figure 6c), while the peak stays unchanged with 6 equiv of perphenazine (Figure 6d). These CD results demonstrate that the structural changes of Aβ_{40} are expedited by PEI and PEI-P-4.5 but hindered by perphenazine. In addition, Figure 6c−d show that no peaks corresponding to the β-sheet formation appear in the CD spectra after 45 h of incubation, suggesting the absence of mature fibrils. These results validate the ThT assays and AFM studies described above and demonstrate the inhibitory effects of PEI-P-4.5 and perphenazine on Aβ_{40} aggregation. The CD results over time (Figure 6c) support that PEI-P-4.5 is able to promote the early structural transformation during Aβ_{40} aggregation and inhibit fibrillation. PEI accelerates Aβ_{40} aggregation but shows weak β-sheet characteristics in the CD spectrum (Figure 6b), which is consistent with AFM studies. AFM images (Figure 3e) indicate that PEI redirects Aβ aggregation to form disordered aggregates without perfect β-sheet structures. We also conducted the dynamic light scattering (DLS) study to investigate the

DOI: 10.1021/jacs.5b01651
J. Am. Chem. Soc. 2015, 137, 8062−8068

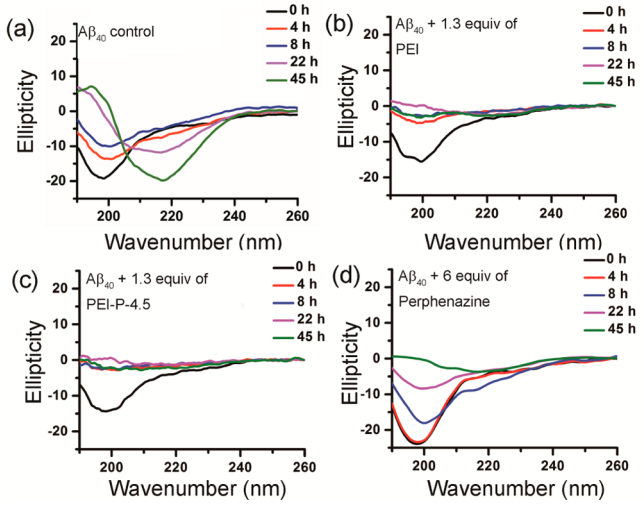

Figure 6. CD spectra. Fibrillation kinetics of Aβ_{40} (50 μM) monitored by CD without modulators (a), and with 65 μM of PEI, 1.3 equiv (b), 65 μM of PEI-P-4.5, 1.3 equiv (c), and 300 μM of perphenazine, 6 equiv (d). CD measurements were performed after 0, 4, 8, 22, and 45 h of incubation of Aβ_{40} (50 μM) in the absence and presence of PEI, perphenazine, or PEI-P-4.5 in a 10 mM sodium phosphate buffer (pH 7.4) with continuous shaking (100 rpm) at 37 °C. We define equiv as the molar ratio of PEI oligomer, perphenazine, or PEI-P-4.5 oligomer to Aβ_{40}.

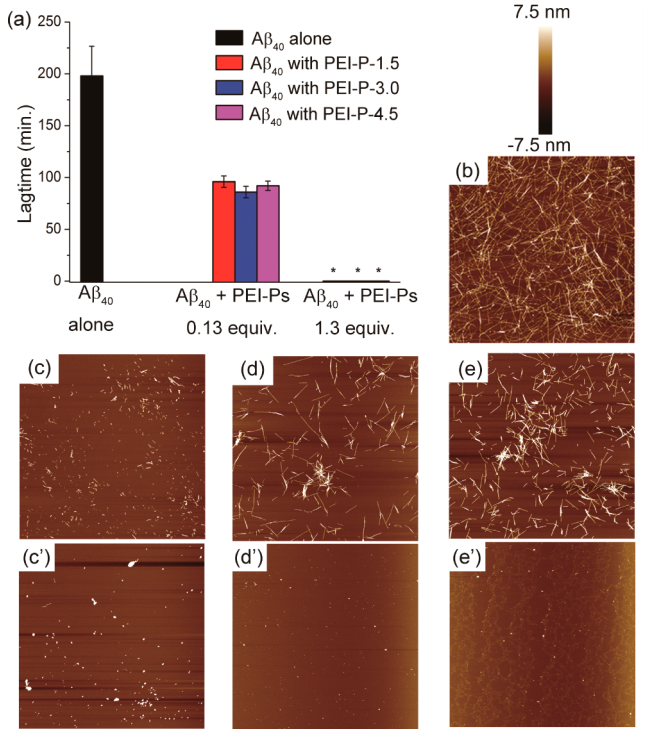

Figure 7. Lag time of Aβ_{40} aggregation without or with modulators monitored by ThT fluorescence assays (a). ThT assays were performed on 15 μM Aβ_{40} peptide in HEPES buffer (pH 7.4) at 37 °C with a shaking speed of 567 rpm. For the complete ThT curves in the full time course, see Figure S33. AFM images of Aβ_{40} (15 μM) after incubation for 20 h without modulators (b), and with 1.95 μM of PEI-P-1.5 after incubation for 20 h, 0.13 equiv (c), 1.95 μM of PEI-P-3.0 after incubation for 20 h, 0.13 equiv (d), 1.95 μM of PEI-P-4.5 after incubation for 20 h, 0.13 equiv (e), 19.5 μM of PEI-P-1.5 after incubation for 20 h, 1.3 equiv (c′), 19.5 μM of PEI-P-3.0 after incubation for 20 h, 1.3 equiv (d′), and 19.5 μM of PEI-P-4.5 after incubation for 20 h, 1.3 equiv (e′). Samples for AFM studies were taken directly from the ThT assays. Image size is 10 × 10 μm^2. We define equiv as the molar ratio of PEI-P-1.5 oligomer, PEI-P-3.0 oligomer, or PEI-P-4.5 oligomer to Aβ_{40}. * Aβ_{40} aggregation exhibits no lag phase with 1.3 equiv of PEI-P conjugates. For details, see Figure S33.

modulation effect of the PEI, perphenazine, and PEI-P-4.5 on Aβ_{40} aggregation. From the DLS results, compared to the hydrodynamic diameter of Aβ_{40} itself, the hydrodynamic diameter of Aβ_{40} incubated with PEI and PEI-P-4.5 at 1.3 equiv increases much faster over the incubation time. Meanwhile, the diameter of the mixture of Aβ_{40} incubated with perphenazine has no significant change even after 24 h of incubation (Figure S41). These results indicate that PEI and PEI-P-4.5 accelerate the formation of small, prefibrillar aggregates of Aβ_{40} in the early stage, while perphenazine inhibits the formation of Aβ_{40} aggregates.

To quantitatively monitor the amount of protein that has aggregated (aggregates >30 kDa), we filtered the Aβ_{40} solutions through filters having a 30 kDa cutoff and determined the protein concentration by a BCA protein assay. The BCA protein assay results show that the aggregated fraction (>30 kDa) of Aβ_{40} increase dramatically over the incubation time when Aβ_{40} is incubated with 1.3 equiv of PEI and PEI-P-4.5, which indicate the acceleration of PEI and PEI-P-4.5 (Figure S42).

Modulation of Aβ Aggregation by PEI-P Conjugates with Different Loadings of Perphenazine. To investigate how the inhibitory periphery of PEI-P conjugates affect Aβ aggregation, we synthesized two more conjugates with different loading ratios. According to the characterization by NMR studies, these PEI-P conjugates have an average 1.5 and 3.0 perphenazine unit per PEI chain designated as PEI-P-1.5 and PEI-P-3.0 respectively.

ThT fluorescence assays and AFM studies indicate that the perphenazine loading affects modulation of Aβ_{40} aggregation by the PEI-P conjugates (Figure 7 and Figure S40). The ThT assays show that PEI-P-1.5, PEI-P-3.0, and PEI-P-4.5 accelerate Aβ_{40} aggregation by 52%, 57%, and 54% at 0.13 equiv, decreasing the lag time from 198 min to 96, 86, and 92 min, respectively (Figure 7a). As controls, PEI-P conjugates in the absence of Aβ_{40} have no ThT fluorescence response (Figure S34). Although the ThT assays show the acceleratory effects of all PEI-P conjugates, the AFM studies indicate that PEI-P-1.5 redirects Aβ_{40} aggregation to form disordered aggregates as PEI does (Figure 7c), while PEI-P-3.0 leads to fibrillation of Aβ_{40} similar to the aforementioned PEI-P-4.5 (Figure 7d and 7e). At higher equivalents (1.3 equiv), PEI-P-3.0 exhibits a delayed lag phase like PEI-P-4.5 (Figure S33c′and S33d′), while PEI-P-1.5 shows a fluorescence response without a typical lag phase (Figure S33b′). AFM studies confirm that Aβ_{40} does not form fibrils in the presence of PEI-P-3.0 or PEI-P-4.5 at 1.3 equiv (Figure 7d′ and 7e′), while Aβ_{40} forms disordered aggregates in the presence of 1.3 equiv of PEI-P-1.5 (Figure 7c′). The above-mentioned results suggest that PEI-P-1.5 redirects Aβ_{40} aggregation as PEI does, while PEI-P-3.0 behaves more like PEI-P-4.5.

Detoxification of Aβ_{40} Aggregates by PEI-P Conjugates. To examine the effect of the PEI-P conjugates on the toxicity of Aβ_{40} toward cells, we used MTT (3-(4,5-dimethylthiazol-2yl)-2,5-diphenyltetrazolium bromide) cell viability assays. We first incubated Aβ_{40} without PEI, perphenazine, and PEI-P conjugates to allow prefibrillar Aβ_{40} aggregates

DOI: 10.1021/jacs.5b01651
J. Am. Chem. Soc. 2015, 137, 8062−8068

to form. The MTT assay shows that the preincubated Aβ_{40} alone kills 60% of the PC-12 cells, relative to the control in which the cells are only incubated with HEPES buffer solution (Figure 8). The deaths of PC-12 cells incubated with 1 equiv

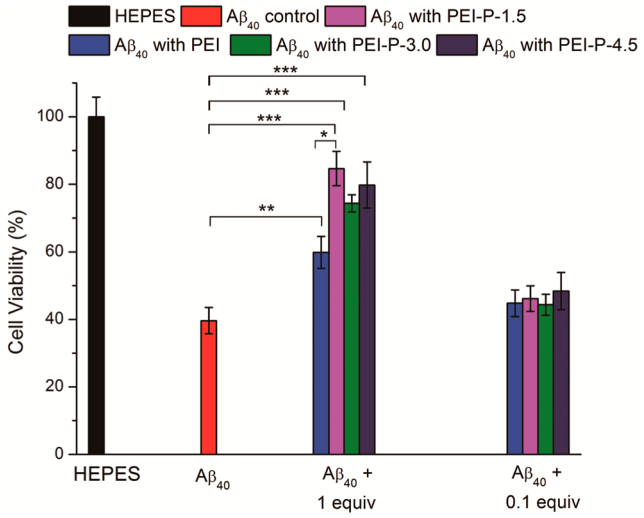

Figure 8. Detoxification of Aβ_{40} aggregates by PEI and PEI-P conjugates. PEI and PEI-P conjugates reduce Aβ_{40} cytotoxicity toward PC-12 cells at different concentrations. Preincubated Aβ_{40} samples with and without PEI or PEI-P conjugates were added to the culture medium of differentiated PC-12 cells. (Final Aβ_{40} concentration is 0.5 μM.) Cell viabilities were measured after incubation for 24 h using MTT assays. The cell survival of the HEPES control is taken to be 100%. Error bars correspond to standard deviations of six sets of experiments. We define equiv as the molar ratio of PEI-P-1.5 oligomer, PEI-P-3.0 oligomer, or PEI-P-4.5 oligomer to Aβ_{40} (Results from t test, $*p < 1 \times 10^{-3}$; $**p < 1 \times 10^{-4}$, $***p < 1 \times 10^{-5}$).

and 0.1 equiv of PEI are 40% and 55%, respectively, which indicates the low detoxification of Aβ_{40} by PEI. The mixtures of PEI and perphenazine also exhibit low detoxification effects (Figure S48). However, the death of PC-12 cells drops to 15%, 26%, and 21%, respecively when Aβ_{40} was preincubated in the presence of PEI-P-1.5, PEI-P-3.0, and PEI-P-4.5 (1.0 equiv). This result indicates that the PEI-P conjugates have the ability to attenuate cytotoxicity caused by Aβ aggregation, and the detoxicification effects are not significantly different among the three conjugates. The MTT assay also shows that the PEI-P conjugates at 0.1 equiv only slightly detoxify the Aβ_{40} aggregates, indicating that the PEI-P conjugates reduce the toxcity of Aβ in a dose-dependent manner. These above-mentioned results from the cell viability assays are not compared with ThT and AFM studies on the modulatory effects of PEI-P conjugates, because detoxification of amyloid aggregation does not necessarily correlate with modulating the pathway of amyloid aggregation. The cytotoxicity of amyloid aggregates depends on the presence of toxic species.[9g]

DISCUSSION

Our studies indicate that the PEI core has the ability to accelerate the formation of the prefibrillar Aβ_{40} intermediates and redirect the aggregation process to form off-pathway disordered aggregates, while perphenazine has the ability to stabilize the on-pathway prefibrillar intermediates, leading to the final fibrils and the delay on pathway aggregation (Figure 9a). It can be imagined that PEI-P conjugates should have the

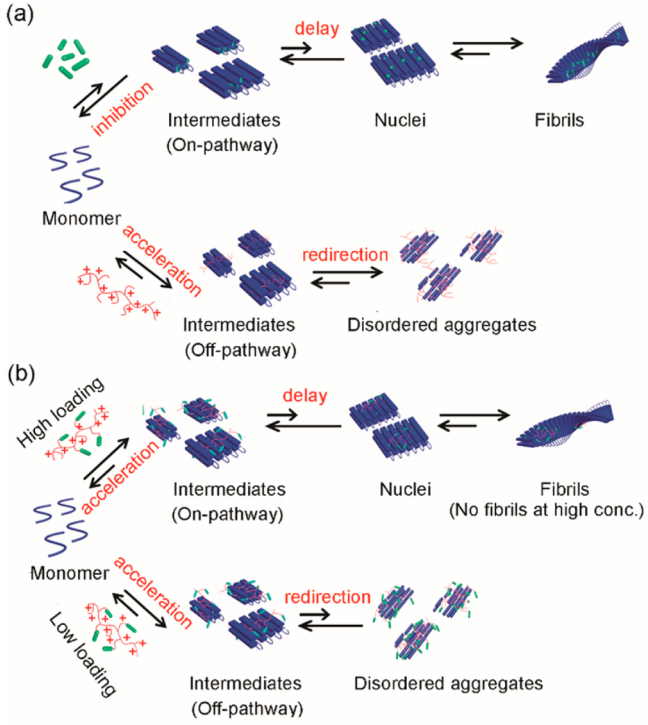

Figure 9. Cartoon representation summarizing modulation of Aβ_{40} aggregation by the PEI-P conjugates, PEI, and perphenazine. (a) On-pathway inhibition of Aβ_{40} aggregation by perphenazine and off-pathway acceleration of Aβ_{40} aggregation by PEI. (b) Loading-dependent modulation of Aβ_{40} aggregation by the PEI-P conjugates.

ability to accelerate, redirect, and delay Aβ_{40} aggregation. Furthermore, the stabilizing and inhibitory abilities of PEI-P conjugates from perphenazine should be enhanced because of the multivalent effect. Accordingly, the loading-dependent and dose-dependent dual effect of PEI-P conjugates on Aβ_{40} aggregation may come from the interplay of the abilities of acceleration (PEI), redirection (PEI), enhanced stabilization (perphenazine and multivalency), and enhanced inhibition (perphenazine and multivalency).

It is surprising that the PEI-P conjugates with a high loading of perphenazine exhibit an on-pathway dual effect on Aβ_{40} aggregation, leading to the formation of Aβ_{40} fibrils, while exhibiting an off-pathway dual effect for PEI-P conjugates with a low loading of perphenazine, entirely redirecting the aggregation process to form disordered Aβ_{40} aggregates, which may be due to the dominated effect of the PEI core (Figure 9b).

Since it has been known that the concentration of amyloid monomers dramatically affects the aggregation process, changes in Aβ_{40} monomer concentrations caused by the applied dosage of the PEI-P conjugates may also play a key role in the dose-dependent dual effect. However, we have not systematically studied the concentration dependence of Aβ_{40} in this work.

SUMMARY

PEI-P conjugates successfully lead to a dual "acceleration–inhibition" modulation effect on Aβ aggregation. This observed dual effect comprises acceleration of the Aβ intermediate formation and inhibition of Aβ fibrillation, resulting from the combination of the acceleration and inhibition in PEI-P conjugates. Our studies show that the perphenazine loading

DOI: 10.1021/jacs.5b01651
J. Am. Chem. Soc. 2015, 137, 8062–8068

and the concentration of the PEI-P conjugates are two key factors in the overall modulation of Aβ aggregation. We envision that the concept described herein could be generalized to other structures that exhibit two modes of modulating Aβ aggregation and other amyloid proteins.

■ ASSOCIATED CONTENT

Supporting Information

Experimental procedures and ^{1}H NMR, ^{13}C NMR, FT-IR, ESI-MS, MALDI-MS, ThT, AFM, BCA, DLS, Micro-DSC, zeta potential, and MTT data. The Supporting Information is available free of charge on the ACS Publications website at DOI: 10.1021/jacs.5b01651.

■ AUTHOR INFORMATION

Corresponding Authors

*jsmoore@uiuc.edu

*pinnanc@outlook.com

Author Contributions

†L.Z. and Y.S. contributed equally.

Notes

The authors declare no competing financial interest.

■ ACKNOWLEDGMENTS

Research supported by the U.S. Department of Energy, Office of Basic Energy Sciences, Division of Materials Sciences and Engineering under Award No. DE-FG02-07ER46471. L.Z. acknowledges support from the China Scholarship Council (No. 201206230036).

■ REFERENCES

(1) (a) Whitesides, G. M.; Mathias, J. P.; Seto, C. T. *Science* **1991**, *254*, 1312−1319. (b) Vauthey, S.; Santoso, S.; Gong, H.; Watson, N.; Zhang, S. *Proc. Natl. Acad. Sci. U.S.A.* **2002**, *99*, 5355−5360. (c) Palmer, L. C.; Stupp, S. I. *Acc. Chem. Res.* **2008**, *41*, 1674−1684. (d) Zhao, X.; Pan, F.; Xu, H.; Yaseen, M.; Shan, H.; Hauser, C. A. E.; Zhang, S.; Lu, J. R. *Chem. Soc. Rev.* **2010**, *39*, 3480−3498.

(2) (a) Harper, J. D.; Lansbury, P. T., Jr. *Annu. Rev. Biochem.* **1997**, *66*, 385−407. (b) Stefani, M.; Dobson, C. M. *J. Mol. Med.* **2003**, *81*, 678−699. (c) Chiti, F.; Dobson, C. M. *Annu. Rev. Biochem.* **2006**, *75*, 333−366. (d) Finder, V. H.; Glockshuber, R. *Neurodegener. Dis.* **2007**, *4*, 13−27.

(3) (a) Ross, C. A.; Poirier, M. A. *Nat. Med.* **2004**, *10*, S10−S17. (b) Campioni, S.; Mannini, B.; Zampagni, M.; Pensalfini, A.; Parrini, C.; Evangelisti, E.; Relini, A.; Stefani, M.; Dobson, C. M.; Cecchi, C.; Chiti, F. *Nat. Chem. Biol.* **2010**, *6*, 140−147. (c) Benilova, I.; Karran, E.; De Strooper, B. *Nat. Neurosci.* **2012**, *15*, 349−357.

(4) Lu, J.; Qiang, W.; Yau, W.; Schwieters, C. D.; Meredith, S. C.; Tycko, R. *Cell* **2013**, *154*, 1257−1268.

(5) (a) Sievers, S. A.; Karanicolas, J.; Chang, H. W.; Zhao, A.; Jiang, L.; Zirafi, O.; Stevens, J. T.; Münch, J.; Baker, D.; Eisenberg, D. *Nature* **2011**, *475*, 96−100. (b) Hirabayashi, A.; Shindo, Y.; Oka, K.; Takahashia, D.; Toshima, K. *Chem. Commun.* **2014**, *50*, 9543−9546. (c) Lee, J. S.; Lee, B. I.; Park, C. B. *Biomaterials* **2015**, *38*, 43−49. (d) Sharma, An. K.; Kim, J.; Prior, J. T.; Hawco, N. J.; Rath, N. P.; Kim, J.; Mirica, L. M. *Inorg. Chem.* **2014**, *53*, 11367−11376.

(6) (a) Denny, R. A.; Gavrin, L. K.; Saiah, E. *Bioorg. Med. Chem. Lett.* **2013**, *23*, 1935−1944. (b) Zhang, M.; Mao, X.; Yu, Y.; Wang, C.-X.; Yang, Y.-L.; Wang, C. *Adv. Mater.* **2013**, *25*, 3780−3781.

(7) (a) Berg, T. *Angew. Chem., Int. Ed.* **2003**, *42*, 2462−2481. (b) Dong, J.; Shokes, J. E.; Scott, R. A.; Lynn, D. G. *J. Am. Chem. Soc.* **2006**, *128*, 3540−3542. (c) Fegan, A.; White, B.; Carlson, J. C. T.; Wagner, C. R. *Chem. Rev.* **2010**, *110*, 3315−3336. (d) Song, Y.; Cheng, P.-N.; Zhu, L.; Moore, E. G.; Moore, J. S. *J. Am. Chem. Soc.* **2014**, *136*, 5233−5236.

(8) Härd, T.; Lendel, C. *J. Mol. Biol.* **2012**, *421*, 441−465.

(9) (a) Bard, F.; Cannon, C.; Barbour, R.; Burke, R.-L.; Games, D.; Grajeda, H.; Guido, T.; Hu, K.; Huang, J.; Johnson-Wood, K.; Khan, K.; Kholodenko, D.; Lee, M.; Lieberburg, I.; Motter, R.; Nguyen, M.; Soriano, F.; Vasquez, N.; Weiss, K.; Welch, B.; Seubert, P.; Schenk, D.; Yednock, T. *Nat. Med.* **2000**, *6*, 916−919. (b) Xia, W. *Curr. Opin. Invest. Dr.* **2003**, *4*, 55−59. (c) Stains, C. I.; Mondal, K.; Ghosh, I. *Chem. Med. Chem.* **2007**, *2*, 1674−1692. (d) Mishra, R.; Bulic, B.; Sellin, D.; Jha, S.; Waldmann, H.; Winter, R. *Angew. Chem., Int. Ed.* **2008**, *47*, 4679−4682. (e) Bieschke, J.; Russ, J.; Friedrich, R. P.; Ehrnhoefer, D. E.; Wobst, H.; Neugebauer, K.; Wanker, E. E. *Proc. Natl. Acad. Sci. U.S.A.* **2010**, *107*, 7710−7715. (f) Sievers, S. A.; Karanicolas, J.; Chang, H. W.; Zhao, A.; Jiang, L.; Zirafi, O.; Stevens, J. T.; Munch, J.; Baker, D.; Eisenberg, D. *Nature* **2011**, *475*, 96−100. (g) Cheng, P.-N.; Liu, C.; Zhao, M.; Eisenberg, D.; Nowick, J. S. *Nat. Chem.* **2012**, *4*, 927−933.

(10) (a) Goldstein, G.; Scheid, M. P.; Boyse, E. A.; Schlesinger, D. H.; Van Wauwe, J. *Science* **1979**, *204*, 1309−1310. (b) Lorenzo, A.; Yankner, B. A. *Proc. Natl. Acad. Sci. U.S.A.* **1994**, *91*, 12243−12247. (c) Osborne, M. A.; Zenner, G.; Lubinus, M.; Zhang, X.; Zhou, S.; Cantley, L. C.; Majerus, P.; Burn, P.; Kochan, J. P. *J. Biol. Chem.* **1996**, *271*, 29271−29278. (d) Khajavi, M.; Inoue, K.; Wiszniewski, W.; Ohyama, T.; Snipes, G. J.; Lupski, J. R. *Am. J. Hum. Genet.* **2005**, *77*, 841−850. (e) Porat, Y.; Abramowitz, A.; Gazit, E. *Chem. Biol. Drug Des.* **2006**, *67*, 27−37. (f) Takahashi, T.; Mihara, H. *Acc. Chem. Res.* **2008**, *41*, 1309−1318.

(11) Bieschke, J.; Herbst, M.; Wiglenda, T.; Friedrich, R. P.; Boeddrich, A.; Schiele, F.; Kleckers, D.; Lopez del Amo, J. M.; Grüning, B. A.; Wang, Q.; Schmidt, M. R.; Lurz, R.; Anwyl, R.; Schnoegl, S.; Fändrich, M.; Frank, R. F.; Reif, B.; Günther, S.; Walsh, D. M.; Wanker, E. E. *Nat. Chem. Biol.* **2012**, *8*, 93−101.

(12) (a) Smith, C. K.; Regan, L. *Acc. Chem. Res.* **1997**, *30*, 153−161. (b) Fegan, A.; White, B.; Carlson, J. C. T.; Wagner, C. R. *Chem. Rev.* **2010**, *110*, 3315−3336. (c) Forman, C. J.; Nickson, A. A.; Anthony-Cahill, S. J.; Baldwin, A. J.; Kaggwa, G.; Feber, U.; Sheikh, K.; Jarvis, S.e P.; Barker, P. D. *ACS Nano* **2012**, *6*, 1332−1346. (d) Milroy, L.-G.; Grossmann, T. N.; Hennig, S.; Brunsveld, L.; Ottmann, C. *Chem. Rev.* **2014**, *114*, 4695−4748.

(13) Cheng, P.-N.; Spencer, R.; Woods, J. R.; Glabe, C. G.; Nowick, J. S. *J. Am. Chem. Soc.* **2012**, *134*, 14179−14184.

(14) Luo, J.; Yu, C.-H.; Yu, H.; Borstnar, R.; Kamerlin, S. C. L.; Gräslund, A.; Abrahams, J. P.; Wärmländer, S. K. T. S. *ACS Chem. Neurosci.* **2013**, *4*, 454−462.

(15) Goers, J.; Uversky, V. N.; Fink, A. L. *Protein Sci.* **2003**, *12*, 702−707.

(16) Re, F.; Airoldi, C.; Zona, C.; Masserini, M.; La Ferla, B.; Quattrocchi, N.; Nicotra, F. *Curr. Med. Chem.* **2010**, *17*, 2990−3006.

(17) Wolfe, L. S.; Calabrese, M. F.; Nath, A.; Blaho, D. V.; Miranker, A. D.; Xiong, Y. *Proc. Natl. Acad. Sci. U.S.A.* **2010**, *107*, 16863−16868.

(18) Kelly, S. M.; Jess, T. J.; Price, N. C. *Biochim. Biophys. Acta - Proteins and Proteomics* **2005**, *1751*, 119−139.

(19) Bartolini, M.; Bertucci, C.; Bolognesi, M. L.; Cavalli, A.; Melchiorre, C.; Andrisano, V. *ChemBioChem* **2007**, *8*, 2152−2161.

DOI: 10.1021/jacs.5b01651
J. Am. Chem. Soc. 2015, 137, 8062−8068